

Four recent studies in cytochrome P450 modelings: A stable iron porphyrin coordinated by a thiolate ligand; a robust ruthenium porphyrin–pyridine *N*-oxide derivatives system; polypeptide-bound iron porphyrin; application to drug metabolism studies

Tsunehiko Higuchi^{*}, Masaaki Hirobe

Faculty of Pharmaceutical Sciences, University of Tokyo, 7-3-1 Hongo, Bunkyo-ku, Tokyo 113, Japan

Received 10 April 1996; accepted 21 May 1996

Abstract

(1) A distinctive structural feature of P450 is the unusual thiolate coordination to heme. We have succeeded in the preparation of the first synthetic thiolato–iron porphyrin (**SR** complex) which retains its structure during catalytic oxidation. Experiments using **SR** complex have revealed that the thiolate ligand greatly accelerates the rate of the O–O bond cleavage and its heterolysis even in highly hydrophobic media. (2) Heteroaromatic *N*-oxides were found to be excellent oxidants in the presence of ruthenium porphyrin. 2,6-disubstituted pyridine *N*-oxides plus a catalytic amount of Ru porphyrin oxidized olefins and sulfides to afford epoxides and sulfoxides, respectively, in high yields. The system in the presence of hydrogen halide effectively oxidized unactivated alkanes and arenes to give alcohols (or ketones) and *p*-quinones in high yields with high selectivity and an extremely high catalyst turnover number (up to 1.2×10^5). (3) A polypeptide-bound porphyrinatoiron complex was prepared. The polymer complex exhibited greater P450-like activity than non-bound Fe(TPP)Cl in the oxidation of olefin and aniline derivatives. (4) P450 mimics were applied to drug metabolism studies. These model systems were effective for one-step preparation of unstable metabolic intermediates, ‘candidate metabolites’, and for the discovery of novel modes of metabolism.

Keywords: Cytochrome P450; Porphyrin; Thiolate; Axial ligand; O–O bond; Ruthenium; Pyridine *N*-oxide; Epoxidation; Hydroxylation; Quinone; Polypeptide; Decarboxylation

Cytochrome P450s are ubiquitous enzymes which play important roles in diverse *in vivo* processes. The enzymes catalyze the synthesis of physiologically significant biomolecules including various steroids and prostaglandins, and

are mainly responsible for metabolism of xenobiotics. The mechanism of their catalytic activities and structure–function relationships have been the subject of extensive investigation in the field of biomimetic chemistry (for recent reviews, see Ref. [1]). We have succeeded in the construction of several novel model systems of cytochrome P450, and have employed them in

^{*} Corresponding author.

studies of P450 functions, as well as in synthesis and drug metabolism studies.

We report here our recent results in four areas: synthesis of a unique iron porphyrin coordinated by a thiolate anion and evaluation of the relative effect of the axial thiolate ligand by use of the complex [2]; a highly reactive oxidizing system using heteroaromatic *N*-oxides catalyzed by ruthenium porphyrin [3]; synthesis of polypeptide-bound iron porphyrin and examination of the modifying effect of the macromolecule on P450-like reactivities [4]; the application of appropriately designed P450 mimics to drug metabolism studies [5].

1. Pronounced effects of axial thiolate ligand on the reactivity of iron porphyrin

The distinctive structural features of P450 as a hemoprotein are the unusual thiolate coordination to heme and also the extreme hydrophobicity of its active site. Among many heme enzymes, only P450 can hydroxylate unactivated alkanes and arenes. Our interest has been focused on the relative effect of an axial thiolate ligand on the reactivity of heme in lipophilic media as a model of the P450 pocket. The iron porphyrin ligated by alkylthiolate anion (**SR** complex) prepared by us is a unique model which retains its axial thiolate coordination dur-

ing catalytic oxidation reactions (Fig. 1) [2]. The UV–Vis and EPR spectra, elemental analysis and FAB mass spectra all supported the structure shown in the figure. EXAFS analysis of **SR** complex (Fe^{3+}) indicated an Fe–S bond length of 2.20 Å, which is quite close to that in native ferric P450 enzymes [6]. **SR** complex could be stored at room temperature under air for several months.

1.1. The axial ligand effect on the rate of O–O bond cleavage

To clarify the axial ligand effect on the oxygen activation by P450, which is a multistep reaction, the effect at each step should be evaluated using the **SR** complex. First of all, we examined the catalytic activity of **SR** on the peroxide shunt reaction of P450 using alkyl hydroperoxides and compared it with that of $\text{Fe}(\text{TPP})\text{Cl}$ to investigate the relative effect of a thiolate ligand on O–O bond cleavage. 2,4,6-Tri-*tert*-butylphenol (TBPH) and 1,1-diphenyl-2-picrylhydrazine (DPPH) were chosen as substrates because both are known to trap reactive intermediates with high efficiency to produce almost stoichiometrically the 2,4,6-tri-*tert*-butylphenoxy (TBP) or 1,1-diphenyl-2-picrylhydrazyl (DPP) radical [7]. Toluene was used as the solvent, taking into account the highly hydrophobic environment of the active site of

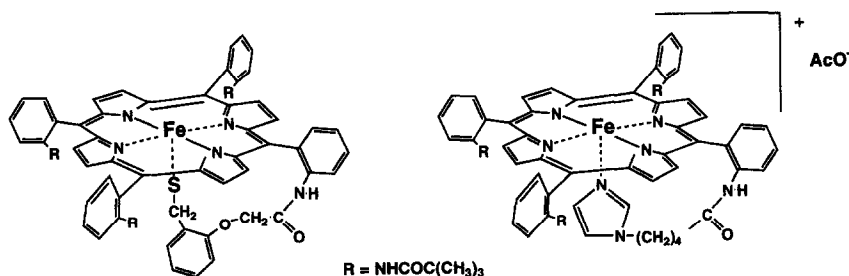


Fig. 1. **SR** complex (left side): UV–Visible spectra of $\text{SR}(\text{Fe}^{\text{II}})\text{--CO}$ complex λ_{max} 383 nm (Soret), 459 nm (Soret). EPR spectra of $\text{SR}(\text{Fe}^{\text{III}})$ at 77 K: g_x 1.96, g_y 2.21, g_z 2.32. Rhombicity = 1.02. XAFS spectra of $\text{SR}(\text{Fe}^{\text{III}})$: Fe–S 2.20 Å, Fe–N 2.00 Å. Elemental analysis. Calcd C: 69.51, H: 5.66, N: 9.40, S: 2.68. Found: C: 69.23, H: 5.52, N: 9.38, S: 2.60. FAB mass spectra ($\text{M} + \text{H}^+$)⁺ 1160. N.P. complex (right side): UV–Visible spectra of $\text{N.P.}(\text{Fe}^{\text{II}})\text{--CO}$ complex λ_{max} 423 nm (Soret). EPR Spectra of $\text{SR}(\text{Fe}^{\text{III}})$ at 77 K. Elemental analysis $g = 6.0, 2.0$. Calcd for $[\text{Fe}(\text{Por})\text{Im}]^+ \cdot \text{AcO}^-$ C: 57.69, H: 5.45, N: 9.34. Found: C: 57.87, H: 5.00, N: 9.27. High-resolution FAB mass. observed m/e 1131.4668 ($\text{M} - \text{OAc}$)⁺. Calcd for $(\text{C}_{67}\text{H}_{67}\text{N}_{10}\text{O}_4\text{Fe})$ 1131.4696.

Table 1

Observed initial rates of TBP· or DPP· formation on the oxidation of TBPH or DPPH with alkyl hydroperoxides catalyzed by SR or FeTPPCL.



Substrate	Oxidant	V (turnover number/min) ^a		V _{SR} /V _{FeTPPCL}
		SR	FeTPPCL	
TBPH	PhC(CH ₃) ₂ OOH	21	0.35	58
	<i>t</i> -Bu-OOH	8.5	0.080	110
DPPH	PhC(CH ₃) ₂ OOH	20	0.085	235
	<i>t</i> -Bu-OOH	7.5	0.041	182

Conditions: solvent = toluene; [TBPH] = 0.2 M; [DPPH] = 0.1 M; [Oxidant] = 5×10^{-2} M; [SR] = [FeTPPCL] = 10^{-4} M. These reactions were carried out at 20° under an argon atmosphere.

^a Observed initial rates of the reactions were based on the catalysts (turnover number of catalysts/min).

P450. EPR spectra of the reaction solution (15 s after the start of the reaction at 25°C) exhibited low-spin spectra of the thiolate-ligated iron porphyrin in addition to the signal of the DPP· formed, and the high-spin signal ($g = 6$) increased very slightly. All of the results supported the conclusion that SR catalyzes the oxidation of the substrates by organic hydroperoxides while the axial thiolate ligand remains essentially unoxidized. Comparison of the rates of the reactions (Table 1; this table is reproduced from Ref. [2]) shows the cytochrome

P450 model SR to have about 60–240 times higher catalytic activity than Fe(TPP)Cl. Thus, the acceleration of the catalytic reaction by thiolate ligation is undoubtedly due to the enhancement of O–O bond scission, because the concentration of the peroxides used in these reactions is so high that the O–O bond cleavage step is rate-determining. The cyclic voltammogram of SR in DMF showed a reversible reduction couple (Fe(III)/Fe(II)) at –0.45 V versus SCE, which is more negative than that for Fe(TPP)Cl (–0.27 V versus SCE) (Table 2).

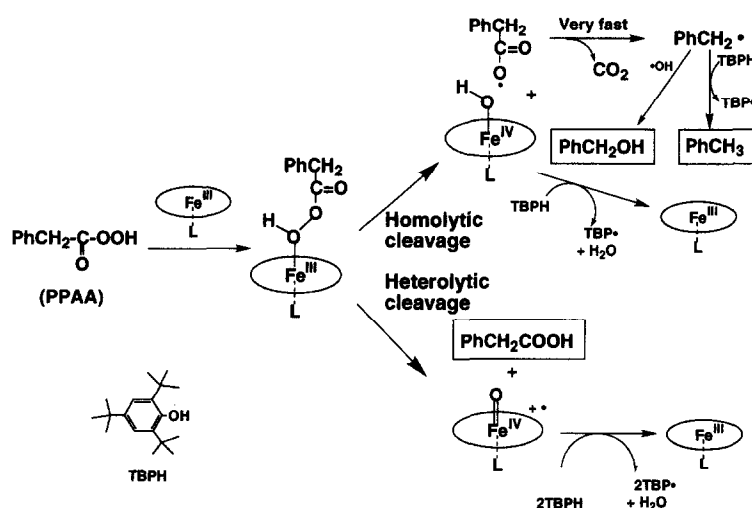


Fig. 2. PPAAs as a probe for the determination of the mode of O–O bond cleavage.

The negativity of the redox potential of **SR** is probably due to electron donation from the thiolate to the iron atom.

1.2. The axial ligand effect on the mode of the O–O bond cleavage

Next, we investigated the effect of thiolate ligand on the mode of the O–O bond cleavage. A new iron porphyrin axially and intramolecularly coordinated by imidazole, termed the **NP** complex, was prepared in order to compare the effect of imidazole as an axial ligand with that of thiolate [8]. The structure of **NP** is a modification of the imidazole-ligated heme prepared by Collman et al. [9]. The UV–Vis and EPR spectra, elemental analysis and high-resolution FAB mass spectra all supported the structure shown in Fig. 1. We compared the catalytic activity of **NP** with that of **SR** complex in an oxidation system using peroxyphenylacetic acid (PPAA). PPAA is a useful probe for the determination of the mode of the O–O bond cleavage, as illustrated in Fig. 2 [10]. **SR** gave PAA quantitatively, while Fe(TPP)Cl mainly catalyzed the formation of toluene, benzyl alcohol, and carbon dioxide (Table 3: this table is reproduced from Ref. [8]). Complex **NP** showed moderate reactivity, intermediate between those of **SR** and Fe(TPP)Cl. Therefore we can unambiguously conclude that **SR** breaks the O–O bond of peroxyacids *heterolytically in benzene*. This result indicates that the thiolate ligand enhances heterolytic cleavage of peroxyacid–iron porphyrin complex even in highly hydrophobic media without the assistance of acid or base. In contrast, it was deduced from our data that Fe(TPP)Cl catalyzes the homolysis of peroxyacid in benzene. The conclusion concerning the O–O bond homolysis by Fe(TPP)Cl in benzene is consistent with the results described by Groves, Watanabe and co-workers [11]. It is expected that a more strongly electron-donating axial ligand would increase both the proportion and rate of heterolytic O–O bond scission.

Table 2

Redox potentials (Pt versus SCE) of the iron porphyrins

Iron porphyrin	Fe(III)P/Fe(II)P	Fe(II)P/Fe(I)P
SR (DMF)	–0.45 (V)	–1.26 (V)
SR (CH ₂ Cl ₂)	–0.54	n.d.
Fe(TPP)Cl(DMF)	–0.27	–1.08

In 0.1 M *n*-Bu₄NClO₄/solvent at Pt versus NaSCE reference. n.d.: not determined.

Therefore, the order of donative character of the examined ligands can be estimated to be as follows: thiolate > imidazole ≫ chloride anion. These results are supported by a related, and independent work [12] which was published in the same year as ours (Ref. [8]). White et al. proposed a mechanism involving homolysis of the O–O bond for P450, based on the result of experiments using the enzyme itself and PPAA as a peroxide probe [10]. They observed benzyl alcohol formation in the oxidation of aliphatic substrates with PPAA catalyzed by P450s. Therefore, the mode of the O–O bond cleavage by P450 remains controversial. Our study using **SR** complex should contribute to the discussion.

Further, the reactivity of the active species formed by cleavage of the O–O bond of peroxyacid–iron porphyrin complexes was examined by using unactivated alkanes as substrates in benzene (Table 3). The **SR** complex catalyzed the hydroxylation of adamantane so efficiently that the yield of adamantanol based on the used *m*CPBA reached 88% (run 1). In the reaction, 80% of **SR** was confirmed to remain undecomposed by EPR and UV–Vis examinations. On the other hand, only a low or moderate yield of adamantanol was obtained by catalysis with Fe(TPP)Cl or **NP**, although *m*CPBA was completely consumed (runs 2, 3). Both Fe(TPP)Cl and **NP** also retained their structures after completion of the reactions. The degree of activity of iron porphyrins for heterolysis of PPAA in benzene is thought to correlate positively with the degree of hydroxylation activity toward alkanes.

Table 3
Oxidation of substrate with peroxyacid catalyzed by iron porphyrins

Run	Iron porphyrin	Substrate	Peroxyacid	Products (yield %) ^a	TBP ^c (kcat = 12.5) ^b TBP (kcat = 0.043) ^b TBP (kcat = 0.33) ^b TBP (kcat = 12.1) ^b TBP (kcat = 0.083) ^b
1	SR	TBPH	PPAA	PAA (100)	PhCH ₂ OH (0)
2	Fe(TPP)Cl	TBPH	PPAA	PAA (7)	PhCH ₂ OH (28)
3	NP	TBPH	PPAA	PAA (58)	PhCH ₂ OH (0)
4	SR	TBPH	PPAA + PAA ^c	PAA (98) ^d	PhCH ₂ OH (0)
5	Fe(TPP)Cl	TBPH	PPAA + PAA ^c	PAA (85) ^d	PhCH ₂ OH (14)
6 ^e	SR	adamantane ^g	mCPBA		1-adamantanol (8)
7 ^e	Fe(TPP)Cl	adamantane ^g	mCPBA		1-adamantanol (9)
8 ^e	NP	adamantane ^g	mCPBA		1-adamantanol (34)
9 ^e	SR	adamantane ^g	PPAA		1-adamantanol (65)
10 ^e	Fe(TPP)Cl	adamantane ^g	PPAA		1-adamantanol (11)

These reactions were carried out in benzene at 25° under argon for 10 min. PPAA: PhCH₂CO₂H; PAA: PhCH₂CO₂H; [Fe(Por)] = 1.0 mM; [peracid] = 0.10 mM; [TBPH] = 10 mM. Benzaldehyde was not detected. Otherwise as noted.

^a Yields are based on the oxidants used. Products were determined by GLC and/or GCMS.

^b kcat: the initial rate of TBP^c formation (turnover number/s).

^c One equivalent amount of PAA to PPAA was added.

^d Yield based on two equivalent amounts to the added PPAA.

^e [Fe(Por)] = [peracid] = 1.0 mM.

^f Ketone form product was not detected in any case.

^g [adamantane] = 0.50 M.

2. Versatile, highly efficient oxidations with heteroaromatic *N*-oxides catalyzed by ruthenium porphyrin

Oxidative functionalization of hydrocarbons is a key area of metalloporphyrin chemistry from the viewpoints of model study of cytochrome P450, and utilization of hydrocarbon resources. Many oxidation systems using metalloporphyrins have been reported for oxidation of hydrocarbons. However, the product yields based on substrate used are too low for synthetic purposes in most cases. We have focused on the development of new metalloporphyrin-catalyzed oxidizing systems to serve this purpose. It is thought to significant which oxidant is chosen as an oxygen atom donor to a metallo-

porphyrin, because the formed highly reactive intermediate, which can hydroxylate unactivated alkanes, would oxidize not only hydrocarbon, but also the oxidant itself. It is therefore considered to be preferable for an oxygen atom donor to have the following properties.

(1) The donor (X–O) should readily react with a metalloporphyrin and form reactive species such as a high-valent oxo–metal porphyrin complex.

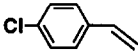
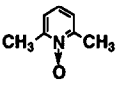
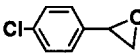
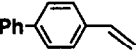
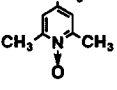
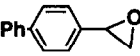

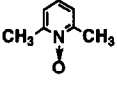
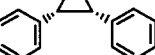
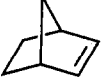
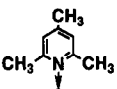

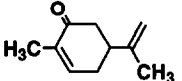
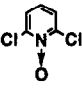
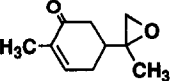
(2) X–O and its deoxygenated product (X) should have only low reactivities toward the formed active intermediate.

(3) X–O and X should be unreactive toward substrates and oxidized products.

(4) The leaving group X should not strongly coordinate to the metal of the catalyst.

Table 4

Epoxidation of various olefins with 2,6-substituted pyridine *N*-oxides catalyzed by Ru(TMP)(O)₂

Olefin	Oxidant	Epoxide	Isolated Yield ^{a)}
			99 %
			92 %
			98 %
			97 % ^{b)}
			70 %

These reaction were carried out in benzene at RT under Ar overnight. [olefin] = 170 mM; [oxidant] = 180 mM; [Ru(TMP)(O)₂] = 0.5–2.0 mM.

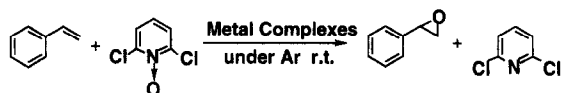
^a Based on olefins.

^b Determined by GLC.

Almost none of the previously reported X–O satisfies all four requirements. We are interested in heteroaromatic *N*-oxides, which are represented by pyridine *N*-oxide derivatives. These *N*-oxides are generally stable at ambient temperature. Pyridine *N*-oxide is unable to oxidize thiols and phosphines at room temperature [13]. Pyridine is resistant to reactive oxidizing reagents such as permanganate, and indeed is frequently used as a solvent in permanganate oxidations. Many nitrogen-containing heterocycles as leaving groups strongly coordinate to metals. However, 2,6-dimethylpyridine has almost no coordinating ability. Therefore, we adopted the *N*-oxides of heterocycles of which the nitrogen atoms are hindered by introducing substituents at the neighboring positions, as candidates for X–O, though heteroaromatic *N*-oxides had not previously been used as effective oxidants for reactions of this kind owing to their

Table 5

The catalytic activity of various metal complexes for the oxygen transfer reactions from pyridine *N*-oxides



Metal complex	Yield ^a	
	epoxide	pyridine
Mn ^{III} (TPP)Cl	0%	0%
Fe ^{III} (TPP)Cl	0	0
Co ^{II} (TPP)	0	0
Mo ^V (TMP)(O)OH	0	0
Ru ^{VI} (TMP)(O) ₂	100	95
Ru ^{VI} (T _{2,6di} FPP)(O) ₂	94 ^b	97 ^b
Ru ^{II} (TPP)CO	26	55
Ru ^{II} (TMP)CO	99	93
Ru ^{II} Cl ₂ (PPh ₃) ₃	0	0
Ru ^{II} Cl ₂ (PPh ₃) ₄	0	0
Rh ^{III} (TMP)Cl	0	0
Rh ^{II} (TMP)	0	0
Os ^{VI} (TMP)(O) ₂	trace	0

[Metal complex] = 1 mM, [styrene] = 170 mM, [2,6-diCl-pyridine *N*-oxide] = 180 mM in benzene under Ar at RT.

^a Based on starting materials.

^b Carried out in CH₂Cl₂.

Table 6

Oxygen atom transfer activity of pyridine *N*-oxide derivatives to Ru porphyrin



Pyridine R ₁	<i>N</i> -oxide R ₂	Time	Pyridine yield ^{a,b}	Epoxide yield ^{a,c}
H	H	o.n. ^d	n.d. ^e	trace
CH ₃	H	o.n.	n.d.	26%
Cl	H	o.n.	100%	94
CH ₃	CH ₃	6 h	n.d.	95
Cl	Cl	2 h	95	100
Br	Br	6 h	100	98
Ph	Ph	o.n.	n.d.	trace

These reactions were carried out in benzene at room temperature under Ar ([olefin] = 170 mM, [pyridine *N*-oxide] = 180 mM, [RuTMP(O)₂] = 1 mM).

^a Detected by GLC.

^b Based on pyridine *N*-oxides.

^c Based on olefins.

^d Overnight (16 ~ 20 h).

^e Not determined.

low oxidation abilities compared to the above oxidants.

2.1. Olefin epoxidation

Among various metalloporphyrins, only ruthenium (Ru) porphyrins are excellent catalysts for transfer of the oxygen atom of *N*-oxide to an olefin [3]. We have found that the Ru porphyrin-2,6-disubstituted pyridine *N*-oxide couple efficiently epoxidizes various olefins (Table 4). No metal complexes examined, except for Ru(por), worked as catalysts (Table 5). An olefin and a slight excess amount of 2,6-dimethylpyridine *N*-oxide were mixed in benzene, then the olefin and the *N*-oxide were completely converted into the epoxide and 2,6-dimethylpyridine by the addition of the catalytic amount (0.5 mol%) of Ru^{VI}(TMP)(O)₂ to the mixture. *cis*-stilbene gave *cis*-stilbene oxide selectively in the reaction. The turnover number reached 17,000. The reaction did not proceed with non-substituted pyridine *N*-oxide, as expected. 2-

Table 7
Reactivity of various heteroaromatic *N*-oxides as oxidants

<i>N</i> -Oxide	Yield of Epoxide	<i>N</i> -Oxide	Yield of epoxide
	95 %		99 %
	100		59
	99		28
	46		

methylpyridine *N*-oxide worked as an oxidant to some extent. 2,6-Disubstituted pyridine *N*-oxide generally had excellent activities to epoxidize olefins quantitatively (Table 6). The only exception was 2,6-diphenylpyridine *N*-oxide, which had almost no oxidizing activity. This inertness is probably due to the steric hindrance by the phenyl groups. The addition of pyridine (only 2 equivalent to Ru(Por)) to the usual system completely inhibited the reaction. Therefore, these results indicate the significance of inhibition by coordination of the formed pyridines. Halogen-substituted pyridine *N*-

Table 9
Selective epoxidation of natural diene acetates

Run	Terpenes	6,7-Epoxide	Yield ^a 2,3-Epoxide	Diepoxide
1		79% ^b (90%) ^c	1% (1%)	3% (3%)
2		75% (78%)	2% (2%)	16% (17%)
3		97% (97%)	0% ^d (0%)	0% (0%)

These reactions were carried out in benzene at room temperature under Ar for 2 d ([terpene] = 170 mM, [lutidine *N*-oxide] = 250 mM, [RuTMP(O)₂] = 1 mM).

^a Determined by 400 MHz NMR.

^b Based on terpenes.

^c Based on conversion.

^d 1,2-epoxide.

oxides had higher reactivity than methyl-substituted ones in terms of yield and reaction rate. *N*-oxides of heteroaromatic compounds other than pyridine are also effective as oxidants, provided that the coordination abilities of their deoxygenated heteroaromatic are sufficiently low (Table 7) [14]. This *N*-oxide/Ru(Por) system stereospecifically epoxidized a *cis*-olefin to afford a *cis*-epoxide (Table 8). Competitive oxidation of *cis*- and *trans*- β -methylstyrene resulted in the selective conversion of *cis*- β -methylstyrene to the *cis*-epoxide. This *cis*-olefin selectivity has also been observed in the study of the Fe(TMP)Cl–PhIO system by Groves and Nemo [15]. Acetates of natural dieneols, i.e., geraniol, linalol, and nerol, were selectively

Table 8
Competitive epoxidation of 1:1 mixture of *cis*- and *trans*-olefin

1 : 1 mixture of <i>cis</i> - and <i>trans</i> -olefin	Yield of epoxide		Recovery	
	87 %	1 %	2 %	99 %
	89 %	5 %	7 %	91 %

These reactions were carried out in benzene at room temperature (stilbene: for 4 h; β -methylstyrene: o.n.) ([*cis*-olefin] = [*trans*-olefin] = [2,6-lutidine *N*-oxide] = 170 mM). Yields were based on used *cis*(*trans*)-olefins.

Table 10
Oxidation of adamantane with Ru porphyrin-2,6-diCl-pyridine *N*-oxide system

Run	Catalyst	Additive	Time	Temp.	Products (% yield) ^{a,b}		
					Adam.-1-ol (a)	Adam.-1,3-diol (b)	Adam.-2-one (c) ⁱ
1	RuTMP(O) ₂	HCl	24 h	r.t.	68	25	1
2	RuTMP(O) ₂	HBr	24 h	r.t.	63	15	2
3	RuTMP(O) ₂	—	24 h	r.t.	4	n.d. ^f	trace ^g
4	—	HCl	24 h	r.t.	1	n.d.	n.d.
6	RuTPP(CO)	HBr	6 h	r.t.	66	27	trace
8 ^{c,d}	RuTPP(CO)	HBr	15 h	40°	66 (6600) ^h	22 (4400)	0.5 (100)
10 ^{c,e}	RuTPP(CO)	HBr	6 h	80°	59 (59,000)	29 (58,000)	1.5 (3000)

These reactions were carried out in benzene under Ar. The reaction mixtures contained adamantane (200 mM), 2,6-dichloropyridine *N*-oxide (260 mM), catalyst (1.0 mM), 36% HCl aq. (200 ~ 410 mM) or 48% HBr aq. (120 ~ 240 mM), and molecular sieves 4A (100 mg/ml).

^a Yields were based on starting adamantane (%).

^b Determined by GLC.

^c [adamantane] = 1.0 M, [N-oxide] = 1.3 M.

^d [catalyst] = 100 μM.

^e [catalyst] = 10 μM.

^f Not detected.

^g < 0.5%.

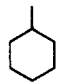
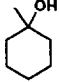
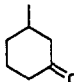
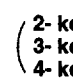
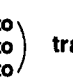
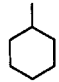
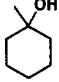
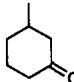
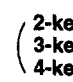
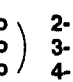
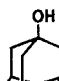
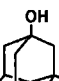
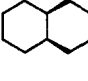
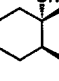
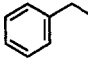
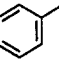
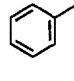
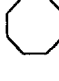
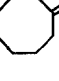
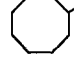
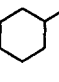
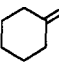
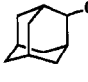

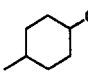
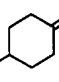
^h The turnover number per catalyst (turns).

ⁱ Adamantan-2-ol was not detected.

mono-epoxidized (Table 9), in all cases, at the 6,7-double bonds. The steric and electronic effects of acetoxy groups may cause the highly selective epoxidation. Sulfides were also oxidized to afford the sulfoxides and the sulfones

in good yields. However, the sulfide oxidation required more time or higher temperature for completion than epoxidation. This retardation is probably attributable to coordination of a sulfide or a sulfoxide to the Ru atom [16,17].

Table 11
Hydroxylation and/or ketonization of various alkanes and alcohols

Run	Substrate	Condition	Product (Yields are based on substrates) ^a
1		cat. = RuTPP(CO) add. = HBr [N-oxide] = 2.0 equiv. r.t., 6 h	 94 %  (2-keto) trace ^d  (3-keto)  (4-keto)
2		cat. = RuTMP(O) ₂ add. = HBr [N-oxide] = 2.2 equiv. 40°, 9 h	 77 %  (2-keto) 2- : 3 %  (3-keto) 3- : 2 %  (4-keto) 4- : 1 %
3		cat. = RuTMP(O) ₂ add. = HBr [N-oxide] = 1.1 equiv. 60°, 4 h	 74 % ^b (90 % ^c)
4		cat. = RuTPP(CO) add. = HBr [N-oxide] = 1.2 equiv. r.t., 6 h	 72 % ^b (80 % ^c)
5		cat. = RuTMP(O) ₂ add. = HCl [N-oxide] = 2.2 equiv. r.t., 24 h	 88 %  n.d. ^e
6		cat. = RuTPP(CO) add. = HBr [N-oxide] = 3.0 equiv. r.t., 40 h	 77 %  2 %
7		cat. = RuTMP(O) ₂ add. = HCl [N-oxide] = 1.1 equiv. r.t., 24 h	 88 %
8		cat. = RuTMP(O) ₂ add. = HBr [N-oxide] = 1.1 equiv. r.t., 24 h	 84 % ^b
9		cat. = RuTMP(O) ₂ add. = HCl [N-oxide] = 1.1 equiv. r.t., 24 h	 81 % ^b

These reactions were carried out under Ar in benzene ([substrate] = 200 mM, [catalyst] = 1 mM, HBr aq. (47%) or HCl aq. (36%) = 30 μl/ml, molecular sieves 4A = 100 mg/ml).

^a Yields are based on substrates (detected by GLC).

^b Isolated yield.

^c Based on conversion.

^d < 0.5%.

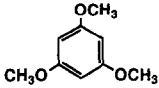
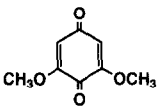
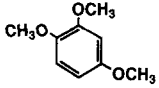
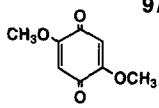
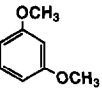
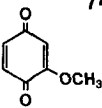
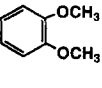
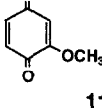
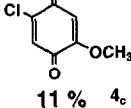
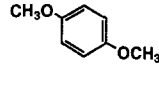
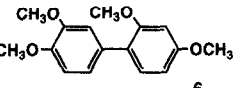
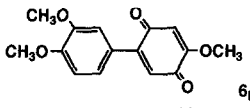
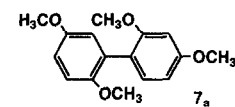
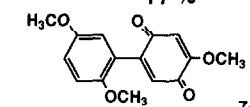
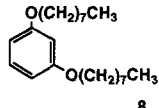
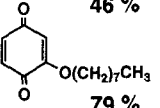
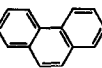
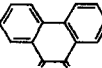
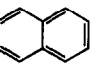
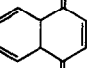
^e Not detected.

2.2. Alkane hydroxylation

We next examined the effect of additives upon the oxidation reactivity of this system,

with the aim of developing a novel oxidation system for alkanes and other unreactive compounds. We found that the catalytic ability of ruthenium porphyrins was enhanced by the

Table 12
Oxidation of aromatic compounds by ruthenium porphyrin-2,6-dichloropyridine *N*-oxide system

1		1 _a	Ru(TPP)CO HBr		1 _b	97 %
2		2 _a	Ru(TPP)CO HBr		2 _b	74 %
3		3 _a	Ru(TMP)CO HBr		3 _b	74 %
4		4 _a	Ru(TMP)(O) ₂ HCl		3 _b	11 %
					4 _c	11 %
5		5 _a	Ru(TPP)CO HBr	No product		
6		6 _a	Ru(TMP)CO HBr		6 _b	77 %
7		7 _a	Ru(TMP)CO HBr		7 _b	46 %
8		8 _a	Ru(TMP)CO HBr		8 _b	79 %
9		9 _a	Ru(TMP)CO HBr		9 _b	40 %
10		10 _a	Ru(TMP)CO HBr		10 _b	29 %

Reaction conditions: substrate (1 mmol); Ru(por) (2 μ mol); 2,6-dichloropyridine *N*-oxide (4 mmol); 40% HBr or 36% HCl (30 μ l); molecular sieve 4A (200 mg); benzene (2 ml) unless otherwise noted.

presence of a small amount of HCl or HBr and that the oxidation of alkanes or aliphatic alcohols with pyridine *N*-oxides was also catalyzed by ruthenium porphyrins with high efficiency in the presence of these acids (Table 10) [18,19]. Under this condition, adamantane was almost wholly consumed to afford adamantan-1-ol, adamantane-1,3-diol, and adamantan-2-one in yields of 68%, 25%, and 1% based on adamantane, respectively (run 1). The role of HBr or HCl has not yet been fully clarified. However, these acids are considered to work as donors of an axial ligand (Br^- or Cl^-) of Ru porphyrin, and also as activators of an active intermediate, by protonation. Details are described in the Mechanistic studies section. Ruthenium catalysts were extremely stable under these conditions. Adamantane was reacted with 2,6-dichloropyridine *N*-oxide in the presence of 1.0×10^{-4} eq. of Ru(TPP)(CO) and HBr at 40°C. The oxidant was almost exhausted in 15 h, at which time the turnover number was 11,100 (run 8). At higher temperature, Ru(TPP)(CO) gave a turnover number of 120,000 during 6 h (run 9). The turnover frequency for the last case was 5.6/s. Several alkanes were oxidized with this system. The results are shown in Table 11. 1-Methylcyclohexanol was selectively obtained with high efficiency in the oxidation of methylcyclohexane (yield = 94%) (run 1). The oxida-

tion of *cis*-decalin proceeded efficiently and *cis*-decalol was isolated in 72% yield (run 4). The stereo isomer, *trans*-decalol, was not detected by GLC analysis. Ethylbenzene was converted into acetophenone in 88% yield (run 5). Cyclooctane, which is less reactive than a tertiary alkane or benzyl alkane, was oxidized to afford cyclooctanone in reasonable yield (yield = 77%) (run 6). Aliphatic alcohols were also oxidized to afford the corresponding ketones (runs 7, 8, 9). These results indicated that the ketones were generated *via* alcohols in the oxidation of secondary alkanes.

2.3. Selective quinone formation by arene oxidation [20]

This highly reactive Ru(Por)-*N*-oxide system was also expected effectively to oxidize rather unreactive aromatic compounds. We examined oxidation of aromatic compounds with the Ru(Por)-2,6-disubstituted pyridine *N*-oxide system in the presence of acid, and found selective quinone formation [20]. Oxidation of various arenes was examined with 2,6-dichloropyridine *N*-oxide catalyzed by Ru(Por) in the presence of hydrogen halide. Alkoxybenzene derivatives were oxidized to afford mainly *p*-benzoquinones in yields that greatly depended upon the structure of the substrates (Table 12). Compound **1_a** gave the best result (**1_b**: 97%). The turnover number of Ru(Por) reached 33,000 in the case of **1_a**. *m*-dimethoxybenzene (abbreviated as *m*-DMB) (**3_a**) was converted into 2-methoxy-*p*-benzoquinone (**3_b**) in good yield (run 3). In contrast, *o*-DMB (**4_b**) afforded **3_b** and the chlorinated quinone **4_c** in low yield (run 4), and *p*-DMB **5_a** gave almost no product (run 5). Competitive oxidation of *m*-DMB and *o*-DMB resulted in an exclusive oxidation of *m*-DMB and recovery of *o*-DMB (Fig. 3). The reaction rate of *m*-DMB was much higher than that of *o*-DMB in the oxidizing system. Therefore, the chemo-selectivity of the oxidizing system was examined by using compounds **6_a** and **7_a**, which possess both *m*-DMB and *o*-DMB or *p*-DMB

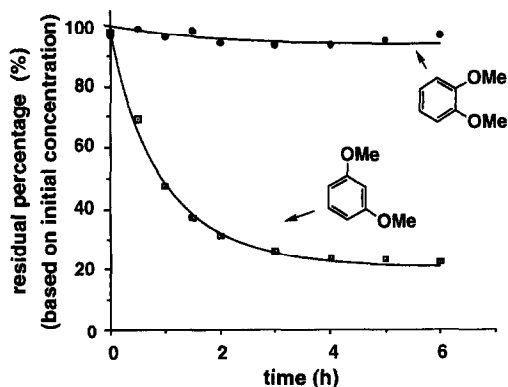


Fig. 3. Competitive oxidation of *o*- and *m*-dimethoxy-benzenes by Ru(TPP)CO-2,6-dichloropyridine *N*-oxide system in the presence of HBr.

structure, as substrates. In the case of **6_a**, 2-methoxy-5-(3,4-dimethoxyphenyl)-*p*-benzoquinone **6_b** was afforded in high yield as a single product (run 6). The oxidation of **7_a** gave an analogous result (**7_b**) (run 7). This type of selectivity is unique among oxidizing reagents commonly used in quinone synthesis (for recent reviews, see Ref. [21]). For example, cerium (IV) ammonium nitrate (CAN) preferentially oxidizes *p*-dimethoxybenzene structures. Our attempt to oxidize **6_a** and **7_a** with CAN resulted in the formation of a complex mixture of products, in each case. The only isolable product in the CAN oxidation of **7_a** was 2-(2,4-dimethoxyphenyl)-*p*-benzoquinone (yield = 8%) as expected.

The hydrocarbon oxidations by the present oxidizing system are the first examples of pyridine N-oxide derivatives working as oxidants in a catalytic oxidation of hydrocarbons.

2.4. Mechanistic studies

In the catalytic reaction with cytochrome P450, iron-oxo porphyrin complexes are considered to be the active intermediates for the

oxidation of substrates (for recent reviews, see Ref. [1]). Since Ru(TMP)(O)₂ was synthesized and characterized by Groves and Quinn [22], this complex has been regarded as analogous to the active intermediate of cytochrome P450, and the oxidation reactivity of this dioxo complex has attracted much interest [22,23]. Considering the difference in reactivity between the Ru(TMP)(O)₂-O₂ system and the Ru(TMP)(O)₂-*N*-oxide system, it seemed likely that some active intermediate other than Ru(TMP)(O)₂ is generated during the oxidation with our system. The rate constant of the reaction between Ru(TMP)(O)₂ and 2-vinylnaphthalene was determined in a mechanistic study [16]. It is clear from the kinetic experiments that the catalytic reaction proceeded at a much faster rate than would be predicted from the reactivity of Ru(TMP)(O)₂, which indicates that an active intermediate other than Ru(TMP)(O)₂ mainly epoxidizes olefins during this catalytic reaction. A study on incorporation of ¹⁸O from labeled water into the epoxide also supported the above proposal [16].

In contrast, it might be possible to understand the mechanism in the presence of HCl or HBr

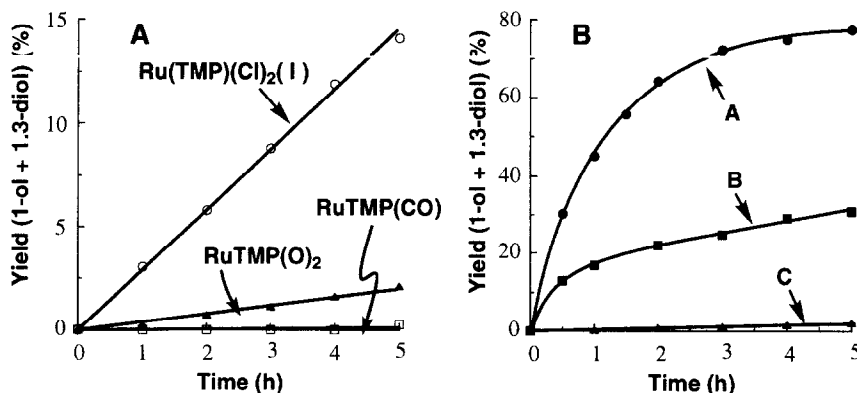


Fig. 4. (A) The hydroxylation of adamantane with 2,6-dichloropyridine *N*-oxide catalyzed by RuTMP(Cl)₂, RuTMP(O)₂, and RuTMP(CO). These reactions were carried out in benzene under Ar at 40°C ([adamantane] = [2,6-dichloropyridine *N*-oxide] = 100 mM, [catalyst] = 0.4 mM). Neither HCl (or HBr) nor molecular sieves were added to the reaction mixtures. Yields (based on starting adamantane) were determined by GLC. (B) The hydroxylation of adamantane with 2,6-dichloropyridine *N*-oxide catalyzed by RuTMP(O)₂ in the presence or the absence of HCl. These reactions were carried out in benzene under Ar at 40°C ([adamantane] = [2,6-dichloropyridine *N*-oxide] = 100 mM, [RuTMP(O)₂] = 0.4 mM). A saturated HCl solution of benzene was added to these reaction mixtures (A: 10 ml/l, B: 5 ml/l, C: 0 ml/l). Molecular sieves were not added to the mixture, because the added HCl solution was anhydrous. Yields (based on starting adamantane) were determined by GLC.

by considering the effect of these acids, because the acids greatly affected the reactivity of the catalytic oxidation. To elucidate the effect of HCl, Ru(TMP)(O)₂ was allowed to react with HCl without substrate or oxidant, and the resulting ruthenium porphyrin complex (**I**) was isolated (y. 82%). It is probable that **I** is the *trans*-dichloro complex of ruthenium porphyrin, formulated as Ru(TMP)(Cl)₂, as judged from its NMR data [19].

The catalytic abilities of a series of complexes, **I**, Ru(TMP)(O)₂, and Ru(TMP)(CO), were compared in the absence of HCl or HBr at 40°C. As shown in Fig. 4, **I** was the most efficient catalyst among them, suggesting that Ru(TMP)(O)₂ and Ru(TMP)(CO) acted as efficient catalysts after conversion into **I** or into complexes which could be generated more easily from **I** than from Ru(TMP)(O)₂ or Ru(TMP)(CO). However, the oxidation with Ru(TMP)(O)₂ in the presence of HCl at 40°C proceeded far more efficiently than that with **I** in the absence of acid, and the amount of added HCl affected the efficiency of the oxidations

(Fig. 4). It is probable that the active intermediates are the ruthenium–oxo porphyrin complexes formulated as [O=Ru^V(por)(X)] (X = Cl or Br) (b), and the acids accelerate the formation of the Ru–oxo intermediate from the *N*-oxide and ruthenium porphyrin in reduced form. The present results do not allow us to identify the mechanism or the active intermediate. Nevertheless, the catalytic activity of ruthenium porphyrins appears to be influenced drastically by the nature of the axial ligands. Further investigation of the mechanistic details is needed and is in progress in our laboratory.

3. Synthesis of polypeptide-bound iron porphyrin and effect of the macromolecule on P450-like reactivities

We designed a novel polypeptide-bound porphyrinato iron complex to investigate the environmental effect in heme enzyme. This polymer porphyrin (PP), was synthesized from poly- γ -methyl-L-glutamate (MW: 100,000) by cou-

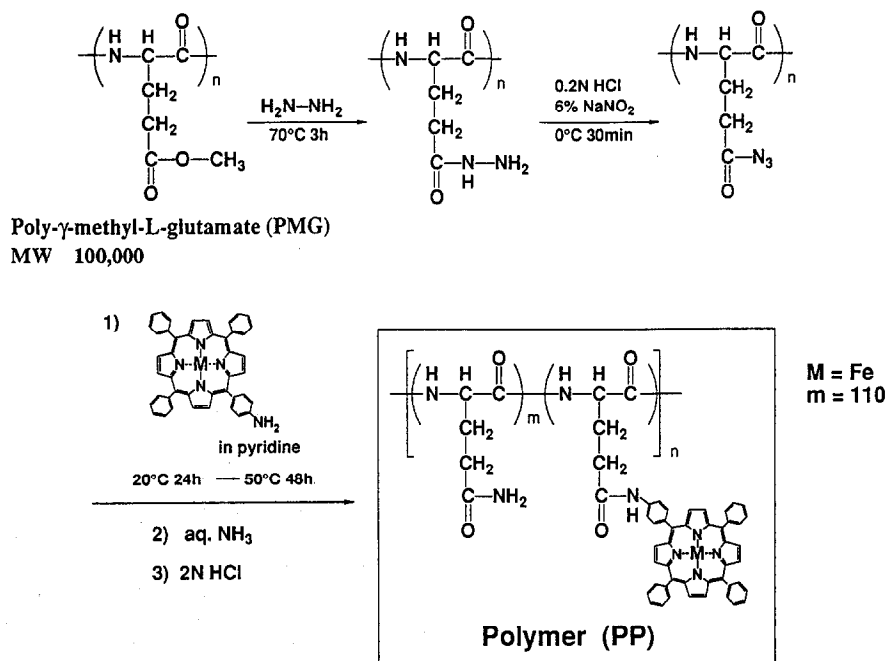


Fig. 5. Synthesis of polypeptide-bound porphyrinatoiron.

pling with $\text{Fe}(\text{TPP})\text{Cl}^4$. The ratio of glutamine residues to $\text{Fe}(\text{TPP})\text{Cl}$ was estimated to be about 110 by atomic absorption analysis (Fig. 5). We have already reported that this polymer complex exhibited more P450-like activities than the non-bound $\text{Fe}(\text{TPP})\text{Cl}$ in the olefin oxidation with molecular oxygen in the presence of NaBH_4 [4].

It is well known that cytochrome P450 catalyzes the demethylation of alkylamines [24]. However, when the described polypeptide-bound porphyrin was used, unexpected products, such as N–N coupling and C–N coupling products, were obtained besides the normal demethylation product, aniline (Table 13) [4]. Table 13 shows the result of this reaction under air in the presence of NaBH_4 . The coupling compounds were produced in relatively high yield compared with the case of the free $\text{Fe}(\text{TPP})\text{Cl}$. Based on this result, we presumed that these products may be unknown metabolites in the P450 system. So we attempted to detect these compounds in a rat liver microsomal reaction mixture using the GC-SIM method [25]. Two rat liver microsomal systems, the NADPH/O_2 and the cumene hy-

droperoxide-supported shunt path, were employed. As expected, these coupling compounds were also found as metabolites of *N*-methyl-aniline in the microsomal system. A significant amount of the coupling product was formed, though the yield was lower than that of the demethylation product.

In addition, P450-specific inhibitors, SKF-525A and metyrapone, suppressed the formation of these coupling products (data not shown). These results indicate that the coupling reaction is P450-dependent. Thus, P450 chemical model systems are available for investigating new metabolic pathways.

4. Application of P450 mimics to drug metabolism studies and evaluation of their utility

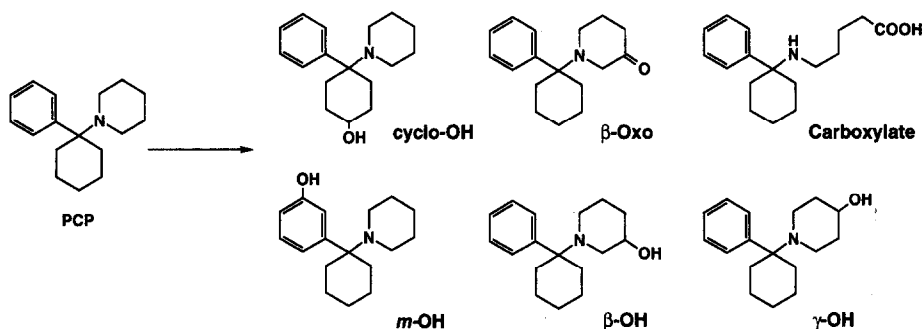
Metabolism of most xenobiotics involves cytochrome P450 in vivo. It is widely recognized that heme in the enzyme is mainly responsible for its chemistry. Chemical models can be useful in studies on drug metabolism, because it is

Table 13
Coupling products formation catalyzed by cyt. P450 model systems

Catalyst	<i>N,N</i>	<i>p-C,N</i>	<i>o-C,N</i> ($\mu\text{mol}/\mu\text{mol cat.}$)	Aniline
Polymer-FeTPPCL	1.84	0.12	1.61	8.92
Free FeTPPCL	0.06	trace	0.12	17.0

The reaction mixture contained catalyst (1 μmol), *N*-methyl-aniline (0.2 mmol), tetramethylammonium hydroxide (0.2 ml of 10% methanol solution), NaBH_4 (0.5 mmol), and methanol (1.3 ml). The reaction mixture was stirred vigorously under air for 3 h at RT.

Table 14
Oxidation of PCP by iron porphyrin–*m*CPBA system



Catalyst	Yield (based on oxidant)					
	<i>m</i> -OH	β -OH	γ -OH	cyclo-OH	β -oxo	carboxylate
SR	n.d.	1.85%	41%	0.44%	18.5%	n.d.
NP	n.d.	2.7	41	0.59	0.41	6.5%
Fe(TPP)Cl	n.d.	0.18	22	0.75	1.2	trace

Reaction conditions; [cat.] = 1 mM, [*m*CPBA] = 1 mM, [PCP] = 500 mM at RT under argon.

usually laborious and expensive to obtain sufficient amounts of drug metabolites by using animals, during the development of new medicines. Some oxidation products identical with metabolites are expected to be afforded by the catalytic oxidation of drugs with metalloporphyrin systems, since their reactivities are thought to resemble, at least to some extent, that of cytochrome P450. The advantages of using model systems to understand drug metabolism are as follows: (1) metabolite candidates can be obtained in relatively large amounts and used to identify the real *in vivo* metabolites and provide samples for pharmacological testing; (2) the mode of metabolism can be clarified, for example, unstable metabolites can be isolated under selected and controlled reaction conditions; and (3) the usage of experimental animals can be reduced.

As the first example for study, we chose the anesthetic agent phencyclidine (PCP), because,

despite being a small molecule, it has an aromatic ring, an aliphatic ring and an N-containing heterocyclic ring moiety, and is expected to exhibit a diversity of reactions in various model systems. As shown in Table 14, many types of oxidation products were produced by using various chemical model systems; phenolic, alcoholic, and ring-opened amino acids [5].

The **SR** and **NP** complexes gave similar products in combination with *m*CPBA as shown in Table 14. It is noteworthy that the piperidine 3-oxo compound was predominantly obtained in the **SR** catalyst system.

We then examined the reaction of PCP in the liver microsomal systems (data not shown). Microsomes–oxidant systems were constituted from three kinds of rat liver microsomes, i.e., non-treated, phenobarbital (PB)-treated and 3-methylcholanthrene (3MC)-treated, as well as non-treated mouse liver microsomes, and two kind of oxidants, cumene hydroperoxide (A)

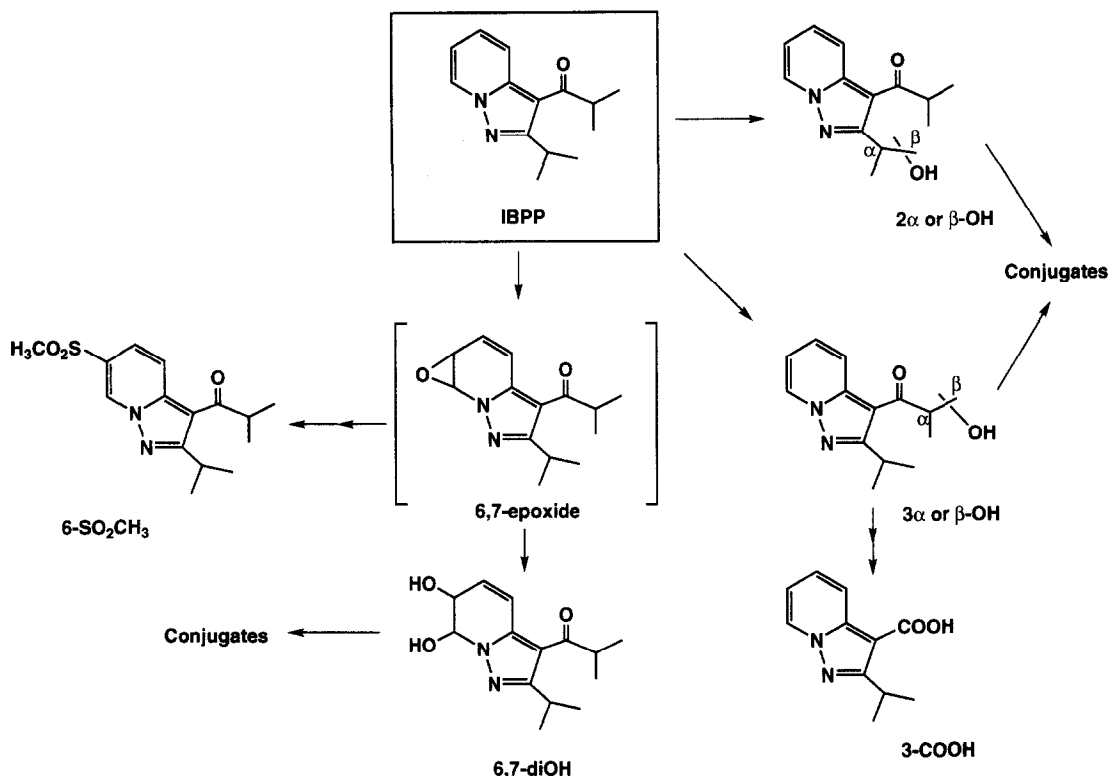


Fig. 6. Metabolic pathways of 3-isobutyl-2-isopropylpyrazolo[1,5-a]pyridine (IBPP) in humans and animals.

and iodoxyllylene (B). The identity of all products (Table 14) was confirmed by comparison with authentic samples obtained from the chemical model systems. The piperidine- β -oxo compound was generated, as in the chemical model systems.

Next, we examined the reaction profiles of the antiasthma drug, IBPP, in various P450 chemical model systems and compared them with those of the rat or human liver microsomal

system. The company involved in this project had difficulty in developing this drug because of the diversity of its metabolic pathways including an unstable metabolite. The metabolic pathways of IBPP *in vivo* are shown in Fig. 6 [26]. The main metabolite is the 6,7-diol, but the 6,7-epoxide, presumed to be its precursor, could not be isolated. However, the epoxide could be obtained in good yield by using the Mn(TPP)Cl/NaOCl system [26] as shown in

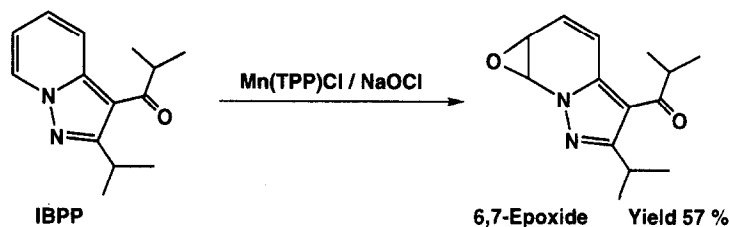


Fig. 7. Synthesis of 6,7-epoxy-IBPP by a Cyt. P450 model.

The inhibitory activities of compound **II_b** and **II_c** on arachidonic acid-induced platelet aggregation in rabbits, though less than those of the mother compounds, were still significant.

Further, we have found that γ,δ - and β,γ -unsaturated carboxylic acids afford δ -hydroxy- γ -lactone and β -hydroxy- γ -lactone, respectively, in one step with the iron porphyrin-iodosylbenzene (PhIO) system (Fig. 10). This type of lactonization has not previously been reported as far as we know. We have also revealed an apparently general metabolic reaction affording γ -lactone compounds from the corresponding γ,δ - and β,γ -unsaturated carboxylic acids, catalyzed by cytochrome P450. Details of this study will be presented in another paper [31].

In summary, we have developed the **SR** complex having axial thiolate as a structural model of the cytochrome P450 active site, a robust and potent Ru porphyrin-heteroaromatic *N*-oxide system as a functional P450 model, and a polypeptide-bound iron porphyrin exhibiting effects due to the macromolecule, and we have applied P450 mimics to drug metabolism studies. We shall be well pleased if these studies contribute to the development of metalloporphyrin chemistry and also the understanding of P450 chemistry.

Acknowledgements

We are grateful to all the co-workers who participated in our P450-modeling studies.

References

- [1] P. Ortiz de Montellano, ed., *Cytochrome P450* (Plenum, New York, 1986); B. Meunier, *Chem. Rev.* 92 (1992) 1411.
- [2] T. Higuchi, S. Uzu and M. Hirobe, *J. Am. Chem. Soc.* 112 (1990) 7051–7053.
- [3] T. Higuchi, H. Ohtake and M. Hirobe, *Tetrahedron Lett.* 30 (1989) 6545.
- [4] T. Mori, T. Santa and M. Hirobe, *Tetrahedron Lett.* 26 (1985) 5555.
- [5] H. Masumoto, K. Takeuchi, S. Ohta and M. Hirobe, *Chem. Pharm. Bull.* 37 (1989) 1788.
- [6] T.L. Poulos, B.C. Finzel and A.J. Howard, *J. Mol. Biol.* 195 (1987) 687.
- [7] T.G. Traylor, W.A. Lee and D.V. Stynes, *J. Am. Chem. Soc.* 106 (1984) 755; L.C. Yuan and T.C. Bruice, *J. Am. Chem. Soc.* 108 (1986) 1643.
- [8] T. Higuchi, K. Shimada, N. Maruyama and M. Hirobe, *J. Am. Chem. Soc.* 115 (1993) 7551–7552.
- [9] J.P. Collman, J.I. Brauman, K.M. Doxsee, T.R. Halbert, E. Bunnenberg, R.E. Linder, G.N. LaMar, J.D. Gaudio, G. Lang and K. Spartalian, *J. Am. Chem. Soc.* 102 (1980) 4182.
- [10] R.E. White, S.G. Sligar and H.J. Coon, *J. Biol. Chem.* 255 (1980) 11108.
- [11] J.T. Groves and Y. Watanabe, *J. Am. Chem. Soc.* 110 (1988) 8443; Y. Watanabe, K. Yamaguchi, I. Morishima, K. Takehira, M. Shimizu, T. Hayakawa and H. Orita, *Inorg. Chem.* 30 (1991) 2582.
- [12] K. Yamaguchi, Y. Watanabe and I. Morishima, *J. Am. Chem. Soc.* 115 (1993) 4058.
- [13] E. Ochiai, *Aromatic Amine Oxides* (Elsevier, Amsterdam, 1967); A.R. Katritzky and J.M. Lagowski, *Chemistry of the Heterocyclic N-oxides* (Academic, London, New York, 1971) ch. III-2, and references cited therein.
- [14] T. Higuchi, H. Ohtake and M. Hirobe, *Tetrahedron Lett.* 32 (1991) 7435.
- [15] J.T. Groves and T.E. Nemo, *J. Am. Chem. Soc.* 105 (1983) 5786.
- [16] H. Ohtake, T. Higuchi and M. Hirobe, *Tetrahedron Lett.* 33 (1992) 2521.
- [17] N. Rajapakse, B.R. James and D. Dolphin, *Catal. Lett.* 2 (1989) 219.
- [18] H. Ohtake, T. Higuchi and M. Hirobe, *J. Am. Chem. Soc.* 114 (1992) 10660.
- [19] H. Ohtake, T. Higuchi and Hirobe, *Heterocycles* 40 (1995) 867.
- [20] T. Higuchi, C. Satake, M. Hirobe, *J. Am. Chem. Soc.* 117 (1995) 8879.
- [21] P.J. Dudfield, in: *Comprehensive Organic Synthesis*, ed. B.M. Trost, Vol. 7 (Pergamon Press, Oxford, 1991) ch. 2.10–2.11.
- [22] J.T. Groves and R. Quinn, *Inorg. Chem.* 23 (1984) 3844; J.T. Groves and R. Quinn, *J. Am. Chem. Soc.* 107 (1985) 5790.
- [23] W.-H. Leung and C.-M. Che, *J. Am. Chem. Soc.* 111 (1989) 8812.
- [24] P.F. Hollenberg, *FASEB J.* 6 (1992) 686, and references cited therein.
- [25] T. Doi, T. Mori, T. Mashino and M. Hirobe, *Biochem. Biophys. Res. Commun.* 191 (1993) 737.
- [26] I. Tabushi and N. Koga, *Tetrahedron Lett.* (1979) 3681; E. Guilmet and B. Meunier, *Tetrahedron Lett.* (1980) 4449.
- [27] Y. Nagatsu, T. Higuchi and M. Hirobe, *Chem. Pharm. Bull.* 37 (1989) 1410.
- [28] Y. Nagatsu, T. Higuchi and M. Hirobe, *Chem. Pharm. Bull.* 38 (1990) 400.
- [29] M. Komuro, Y. Nagatsu, T. Higuchi and M. Hirobe, *Tetrahedron Lett.* 33 (1992) 4949.
- [30] M. Komuro, T. Higuchi and M. Hirobe, *Bioorg. Med. Chem.* 3 (1995) 55–65.
- [31] M. Komuro, T. Higuchi and M. Hirobe, *J. Chem. Soc., Perkin Trans. 1*, in press.